Solar Energy Materials & Solar Cells 95 (2011) 586–594

Contents lists available at ScienceDirect

Solar Energy Materials & Solar Cells

journal homepage: www.elsevier.com/locate/solmat

Simple, fast and accurate two-diode model for photovoltaic modules

Kashif Ishaque *, Zainal Salam, Hamed Taheri

Faculty of Electrical Engineering, Universiti Teknologi Malaysia, UTM 81310, Skudai, Johor Bahru, Malaysia

ARTICLE INFO

Article history:
Received 9 April 2010
Received in revised form
23 July 2010
Accepted 20 September 2010
Available online 20 October 2010

Keywords:
PV module
Multi-crystalline
Mono-crystalline
Thin-film
STC

ABSTRACT

This paper proposes an improved modeling approach for the two-diode model of photovoltaic (PV) module. The main contribution of this work is the simplification of the current equation, in which only four parameters are required, compared to six or more in the previously developed two-diode models. Furthermore the values of the series and parallel resistances are computed using a simple and fast iterative method. To validate the accuracy of the proposed model, six PV modules of different types (multi-crystalline, mono-crystalline and thin-film) from various manufacturers are tested. The performance of the model is evaluated against the popular single diode models. It is found that the proposed model is superior when subjected to irradiance and temperature variations. In particular the model matches very accurately for all important points of the *I–V* curves, i.e. the peak power, short-circuit current and open circuit voltage. The modeling method is useful for PV power converter designers and circuit simulator developers who require simple, fast yet accurate model for the PV module.

1. Introduction

Photovoltaic (PV) power system is a popular renewable energy source due to the absence of moving parts and therefore almost maintenance free. The main component of the system, i.e. the PV module utilizes standard semiconductor processes that can be fabricated with relatively minimum facilities [1]. Furthermore, the power converters (DC–DC converter and/or inverter) that interface the modules with the grid or batteries are well established technologies. However, in a PV power generation, due to the high cost of the modules, optimal use of the available solar energy has to be ensured. This necessitates an accurate simulation model of the PV system, especially the modules.

PV module modeling primarily involves the estimation of the non-linear *I–V* curves. Previous researchers have utilized circuit topologies to model the characteristics of the module when subjected to environmental variations such as changed in irradiance and temperature. By far, the simplest approach is the single diode model i.e. a current source in parallel to a diode [2,3]. An improved version is the inclusion of one series resistance to the circuit, R_s [4–8]. Although the model is still relatively simple, it exhibits serious deficiencies when subjected to high temperature variations because it does not account for the open circuit voltage coefficient, K_V [5]. An extension of the single diode model which includes an additional shunt resistance, R_p is suggested by numerous authors [9–12]. Including R_p, the number of parameters is increased to five. Using this model, the accuracy is improved.

The single diode models were based on the assumption that the recombination loss in the depletion region is absent. In a real solar cell, the recombination represents a substantial loss, which cannot be adequately modeled using a single diode. Consideration of this loss leads to a more precise model known as the two-diode model [13]. However, the inclusion of the additional diode increases the parameters to seven (new parameters: I_{o2}, a_2). The main challenge now is to estimate the values of all the model parameters while maintaining a reasonable computational effort.

To determine the parameters for the above-mentioned topologies, various computational methods are proposed. The single diode with R_s-model only requires four parameters, namely short-circuit current (I_{sc}), saturation current (I_o), diode ideality factor (a) and the series resistance, R_s. In [4,7] an iterative programming method is introduced to estimate the values of R_s and a. These values are further refined by interpolation technique [6]. Several numerical algorithms to model the *I–V* curves using single diode with R_p and R_s are proposed; these include resistive-companion method [9], non-linear least square optimization [10] and other iterative solutions described in [11,12]. Although significant improvement over the single diode with R_s-model is obtained, this approach demands more computing effort. Recently, several authors [14–20] use artificial intelligence (AI) such as fuzzy logic [14] and artificial neural network (ANN) [15–20] to model the *I–V* curves. This is a logical approach if one

* Corresponding author. Tel.: +607 5536187; fax: +607 5566272.
E-mail addresses: kashif@fkegraduate.utm.my (K. Ishaque), zainals@fke.utm.my (Z. Salam).

0927-0248/$ - see front matter © 2010 Elsevier B.V. All rights reserved.
doi:10.1016/j.solmat.2010.09.023

were to consider the dependency of solar cell to the environmental variations. Despite the accurate results, the AI techniques require extensive computation. Furthermore, ANN requires large amount of data for training. Among the above-mentioned methods to compute R_s and R_p, the iterative technique proposed in [12] is the most promising. However its accuracy deteriorates at low irradiance, especially in the vicinity of V_{oc}.

For the two-diode model, the Levenberg/Marquardt curve fitting technique is applied to construct the I–V curves [21,22]. In [23], an equivalent Thevenin circuit is derived to estimate the model parameters, whereas in [24], the parameters are calculated as a function of series resistance. However, in all these techniques [21–24] many new additional coefficients are introduced into the equations. Furthermore difficulty arises in determining the initial values of the parameters; in some cases heuristic solutions need to be sought. Another approach to describe the two-diode model is by investigating its physical characteristics such as the electron diffusion coefficient, minority carrier's lifetime, intrinsic carrier density and other semiconductor parameters. Among the more prominent works in this area are the irradiance decay cell analysis method [25], diffusion-current dominant area [26], modified two-diode model [27] and the modified three-diode model [28]. While these models are useful to understand the physical behavior of the cell, information about the semiconductor parameters are not always available in commercial PV datasheets. Furthermore, most of the aforementioned works consider the ideality factors $a_1=1$ and $a_2=2$. Although this assumption is widely used but not always true [29].

From the preceding discussion, it may be concluded that although the two-diode model is a preferable choice in terms of accuracy, its computational requirement is much more demanding compared to the single diode models [21–24]. That makes it less attractive than the latter. Furthermore, modeling using semiconductor approach as described in [25–28] is not suitable due to insufficient information from the module manufacturer. In this paper, an improved modeling technique for the two-diode model is proposed. The main contribution of this work is the simplification of the current equation, in which only four parameters are required. To compute the values of the series and parallel resistances, a simple and fast iterative method is used. The accurateness of the model is verified by applying the model to six PV modules of different types (multi-crystalline, mono-crystalline and thin-film) from various manufacturers. The performances of the model is evaluated against the single diode R_s [5] and R_p [12] models. It is envisaged that the proposed work can be very useful for PV power converter designers and circuit simulator developers who require simple, fast and accurate model for the PV module.

2. Computational methods to determine circuit parameters

2.1. One-diode model

An ideal solar cell consists of a single diode connected in parallel with a light generated current source (I_{PV}) is shown in Fig. 1(a). The single diode model which includes the series resistance, R_s is depicted in Fig. 1(b).

The output current in Fig. 1(b) is $I=I_{PV}-I_D$. It can be written as

$$I = I_{PV} - I_o\left[\exp\left(\frac{V+IR_s}{aV_T}\right)-1\right] \quad (1)$$

where I_{PV} is the current generated by the incidence of light, I_o is the reverse saturation current, V_T ($=N_skT/q$) is the thermal voltage of the PV module having N_s cells connected in series, q is the electron charge (1.60217646×10^{-19} C), k is the Boltzmann constant

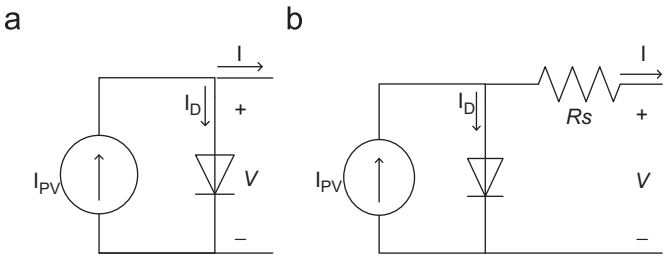

Fig. 1. (a) An ideal solar cell and (b) single diode model with R_s.

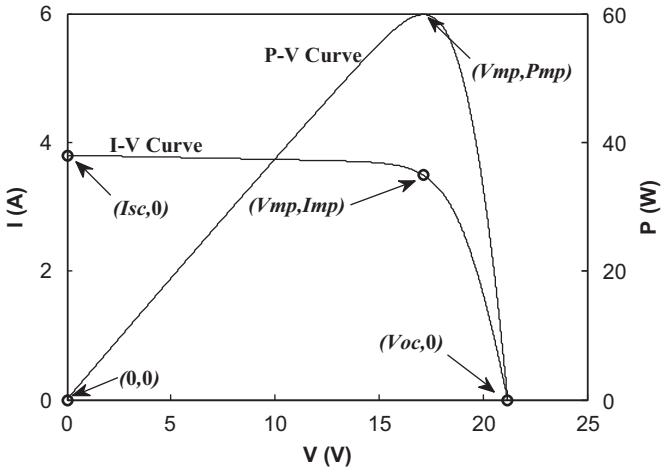

Fig. 2. I–V and P–V characteristic curve.

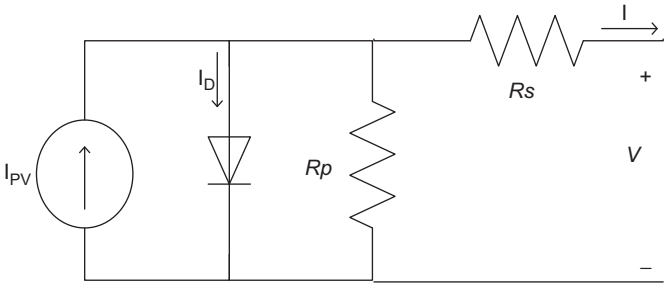

Fig. 3. Single diode model with R_s and R_p.

(1.3806503×10^{-23} J/K), T is the temperature of the p–n junction in K and a is the diode ideality factor. Fig. 2 shows a typical I–V and P–V curves generated from Eq. (1). Typically, three points at standard test conditions (STC) (I_{sc}, 0), (V_{mp}, I_{mp}) and (V_{oc}, 0) are given in the manufacturer's datasheet. An accurate estimation of these points is the main goal of every modeling technique.

Eq. (1) does not adequately represent the behavior of the cell when subjected to environmental variations, especially at low voltage. A more practical model can be seen in Fig. 3, where R_s and R_p represent the series and parallel resistances, respectively. An output current equation using this model can be written as

$$I = I_{PV} - I_o\left[\exp\left(\frac{V+IR_s}{aV_T}\right)-1\right] - \left(\frac{V+IR_s}{R_p}\right) \quad (2)$$

where, R_s and R_p are the equivalent series and parallel resistances, respectively. This model yields more accurate result than the R_s-model, but at the expense of longer computational time.

2.2. Two-diode model

The two-diode model is depicted in Fig. 4 [13]. The following equation describes the output current of the cell:

$$I = I_{PV} - I_{o1}\left[\exp\left(\frac{V+IR_s}{a_1 V_{T1}}\right)-1\right] - I_{o2}\left[\exp\left(\frac{V+IR_s}{a_2 V_{T2}}\right)-1\right] - \left(\frac{V+IR_s}{R_p}\right) \quad (3)$$

where I_{o1} and I_{o2} are the reverse saturation currents of diode 1 and diode 2, respectively, V_{T1} and V_{T2} are the thermal voltages of respective diodes. a_1 and a_2 represent the diode ideality constants. The I_{o2} term in Eq. (3), compensate the recombination loss in the depletion region as described in [13].

Although greater accuracy can be achieved using this model, it requires the computation of seven parameters, namely I_{PV}, I_{o1}, I_{o2}, R_p, R_s, a_1 and a_2. Furthermore I_{o1}, I_{o2}, R_p and R_s, are obtained through iteration. To simplify further, several researchers assumed $a_1=1$ and $a_2=2$. The latter is an approximation of the Schokley–Read–Hall recombination in the space charge layer in the photodiode [13]. Although this assumption is widely used but not always true [29]. As discussed in the introduction section, many attempts have been made to reduce the computational time for the two-diode model. However they appear to be unsatisfactory.

2.3. Determination of two-diode model parameters

In this work, the equation for PV current as a function of temperature and irradiance can be written as [11]

$$I_{PV} = (I_{PV\_STC} + K_I \Delta T)\frac{G}{G_{STC}} \quad (4)$$

where I_{PV_STC} (in ampere) is the light generated current at STC, $\Delta T = T - T_{STC}$ (in Kelvin, $T_{STC}=25\ ^\circ$C), G is the surface irradiance of the cell and G_{STC} (1000 W/m^2) is the irradiance at STC. The constant K_I is the short-circuit current coefficient, normally provided by the manufacturer.

2.3.1. Simplification of saturation current equation

For a single diode model, an improved equation to describe the saturation current which considers the temperature variation is given by [12], i.e.

$$I_o = \frac{(I_{sc\_STC} + K_I \Delta T)}{\exp[(V_{oc,STC} + K_V \Delta T)/aV_T] - 1} \quad (5)$$

The constant K_V is the open circuit voltage coefficient; this value is available from the datasheet.

For the two-diode model, several researchers have calculated the values of I_{o1} and I_{o2} using iteration. The iteration approach greatly increases the computation time, primarily due to the non-suitable values of the initial conditions [30]. In general, I_{o2} is 3–7 orders of magnitude larger than I_{o1}. Furthermore, most of the previous works consider the ideality factors $a_1=1$ and $a_2=2$.

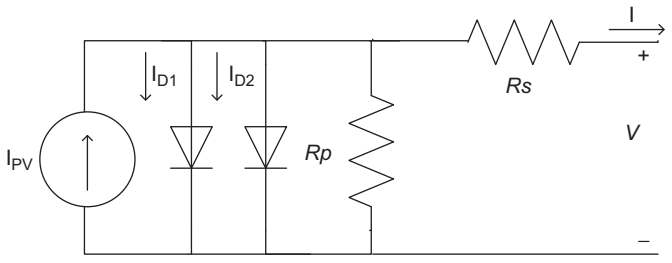

Fig. 4. Two-diode model.

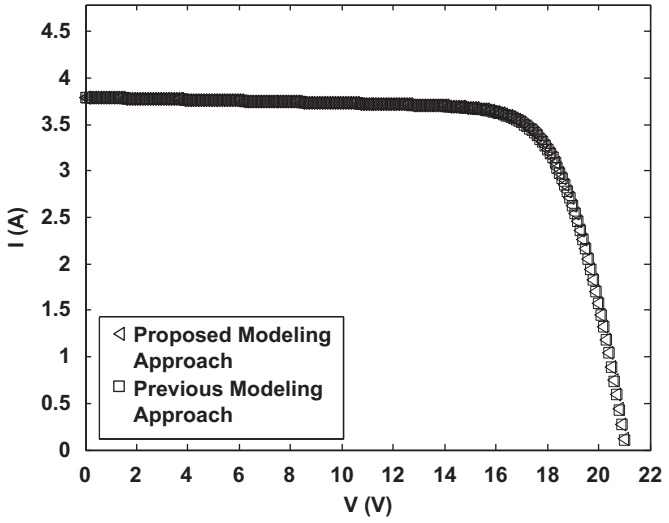

Fig. 5. Comparison of I–V curves for different and equal saturation current (a) Proposed modeling approach: $I_{o1}=I_{o2}=4.7\times10^{-10}$, $R_p=176.4\,\Omega$, $R_s=0.35\,\Omega$ and (b) previous modeling approach: $I_{o1}=4.7\times10^{-10}$, $I_{o2}=2.11\times10^{-6}$, $R_p=200\,\Omega$, $R_s=0.32\,\Omega$.

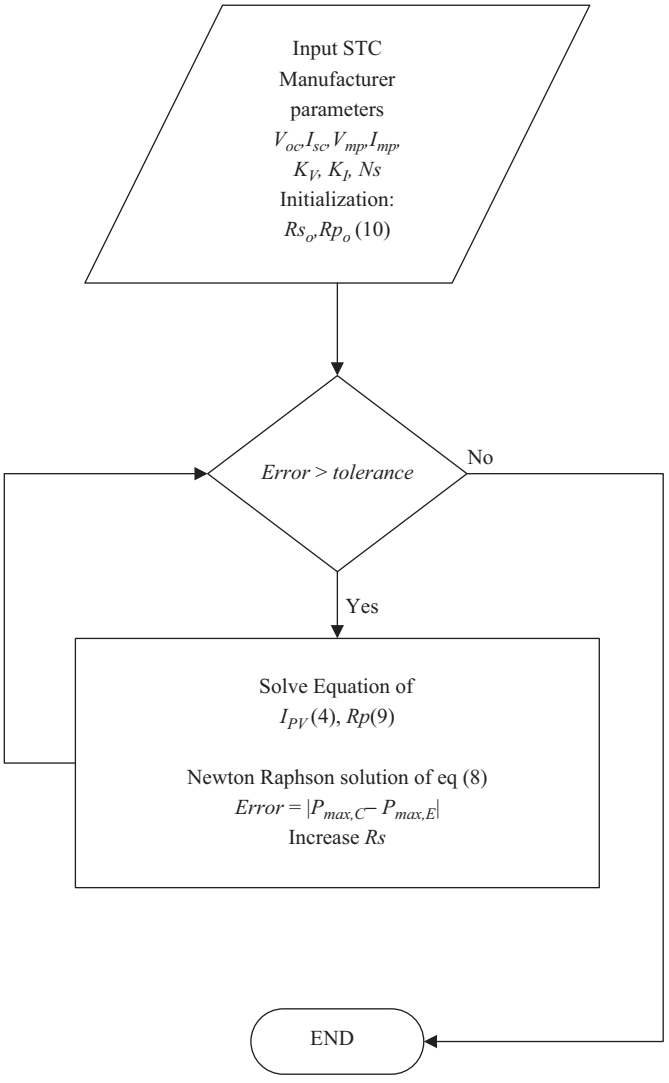

Fig. 6. Matching algorithm.

In this work, we propose a modification of Eq. (5) and apply it to the two-diode model. No attempt has been made to this equation to solve the saturation currents. To maintain the equation in the same form as in Eq. (5), both reverse saturation currents I_{o1}, I_{o2} are set to be equal in magnitude, i.e.

$$I_{o1} = I_{o2} = I_o = \frac{(I_{sc\_STC} + K_I \Delta T)}{\exp[(V_{oc,STC} + K_V \Delta T)/\{(a_1 + a_2)/p\} V_T] - 1} \quad (6)$$

The equalization simplifies the computation as no iteration is required; the solution can be obtained analytically. Diode ideality factors a_1 and a_2 represent the diffusion and recombination current components, respectively. In accordance to Shockley's diffusion theory, the diffusion current, a_1 must be unity [31]. The value of a_2, however, is flexible. Based on extensive simulation carried out, it is found that if $a_2 \geq 1.2$, the best match between the proposed model and practical I–V curve is observed. Since

Table 1
Specifications for the three modules used in the experiments.

Parameter	Multi-crystalline			Mono-crystalline		Thin-film
	BP solar MSX-60	Kyocera KG200GT	Shell S36	Shell SQ150-PC	Shell SP-70	Shell ST40
I_{sc} (A)	3.8	8.2	2.3	4.8	4.7	2.68
V_{oc} (V)	21.1	32.9	21.4	43.4	21.4	23.3
I_{mp} (A)	3.5	7.61	2.18	4.4	4.25	2.41
V_{mp} (V)	17.1	26.3	16.5	34	16.5	16.6
K_V (mV/°C)	−80	−123	−76	−161	−76	−100
K_i (mA/°C)	3	3.18	1	1.4	2	0.35
N_s	36	54	36	72	36	36

Table 2
Parameters for the R_s-model.

Parameter	Multi-crystalline			Mono-crystalline		Thin-film
	MSX-60	KG200GT	S36	SQ150-PC	SP-70	ST40
I_{sc} (A)	3.8	8.21	2.3	4.8	4.7	2.68
V_{oc} (V)	21.1	32.9	21.4	43.4	21.4	23.3
I_{mp} (A)	3.55	7.65	2.16	4.52	4.31	2.5
V_{mp} (V)	17.1	25.6	17.97	36.57	16.73	19.4
I_o (A)	9.094×10^{-8}	2.165×10^{-8}	4.32×10^{-8}	1.562×10^{-8}	9.46×10^{-7}	1.37×10^{-7}
I_{PV} (A)	3.8	8.21	2.3	4.8	4.7	2.68
a	1.2	1.2	1.3	1.2	1.5	1.5
R_s (mΩ)	79	69	14	14	78	16

Table 3
Parameters for the R_p-model.

Parameter	Multi-crystalline			Mono-crystalline		Thin-film
	MSX-60	KG200GT	S36	SQ150-PC	SP-70	ST40
I_{sc} (A)	3.8	8.21	2.3	4.8	4.7	2.68
V_{oc} (V)	21.1	32.9	21.4	43.4	21.4	23.3
I_{mp} (A)	3.5	7.61	2.16	4.4	4.24	2.41
V_{mp} (V)	17.1	26.3	16.7	34	16.5	16.6
I_o (A)	9.094×10^{-8}	9.825×10^{-8}	9.733×10^{-9}	6.975×10^{-8}	8.765×10^{-8}	1.03×10^{-8}
I_{PV} (A)	3.803	8.22	2.301	4.81	4.72	2.70
a	1.3	1.3	1.2	1.3	1.3	1.3
R_p (Ω)	304.83	601.34	4677.8	466.46	122.1	284.1
R_s (Ω)	0.2	0.23	0.73	0.67	0.4	1.52

Table 4
Parameters for the proposed two-diode model.

Parameter	Multi-crystalline			Mono-crystalline		Thin-film
	MSX-60	KG200GT	S36	SQ150-PC	SP-70	ST40
I_{sc} (A)	3.8	8.21	2.3	4.8	4.7	2.68
V_{oc} (V)	21.1	32.9	21.4	43.4	21.4	23.3
I_{mp} (A)	3.5	7.61	2.16	4.4	4.24	2.
V_{mp} (V)	17.1	26.3	16.7	34	16.5	16.6
$I_{o1} = I_{o2}$ (A)	4.704×10^{-10}	4.218×10^{-10}	2.059×10^{-10}	3.106×10^{-10}	4.206×10^{-10}	3.07×10^{-11}
I_{PV} (A)	3.80	8.21	2.3	4.8	4.7	2.68
R_p (Ω)	176.4	160.5	806.4	275	91	211.7
R_s (Ω)	0.35	0.32	0.89	0.9	0.51	1.76

$(a_1+a_2)/p=1$ and $a_1=1$, it follows that variable p can be chosen to be ≥ 2.2. This generalization can eliminate the ambiguity in selecting the values of a_1 and a_2. Eq. (3) can be simplified in terms of p as

$$I = I_{PV} - I_o\left[\exp\left(\frac{V+IR_s}{V_T}\right)+\exp\left(\frac{V+IR_s}{(p-1)V_T}\right)+2\right]-\left(\frac{V+IR_s}{R_p}\right) \quad (7)$$

The simplification of the current equation, i.e. Eq. (7), necessitates for the re-computation of R_p and R_s values. Fig. 5 shows the values of R_p and R_s computed based on Eqs. (3) and (7). It can be seen that for the I–V curve to be identical, values of R_p and R_s are altered accordingly. This shall be explained in the next section.

2.3.2. Determination of R_p and R_s values

The remaining two parameters in Eq. (7), i.e. R_p and R_s are obtained through iteration. Several researchers have evaluated these two parameters independently, but the results are unsatisfactory. In this work, R_p and R_s are calculated simultaneously, similar to the procedure proposed in [12]. This approach has not been applied for two-diode model. The idea is maximum power point (P_{mp}) matching; i.e. to match the calculated peak power ($P_{mp,C}$) and the experimental (from manufacturer's datasheet) peak power ($P_{mp,E}$) by iteratively increasing the value of R_s while simultaneously calculating the R_p value. From Eq. (7) at maximum power point condition, the expression for R_p can be rearranged and rewritten as

$$R_p = \frac{V_{mp}+I_{mp}R_s}{\{I_{PV}-I_o[\exp((V_{mp}+I_{mp}R_s)/V_T)+\exp((V_{mp}+I_{mp}R_s)/(p-1)V_T)+2]-P_{\max,E}/V_{mp}\}} \quad (8)$$

The initial conditions for both resistances are given below

$$R_{so}=0; \quad R_{po}=\frac{V_{mp}}{I_{scn}-V_{mp}}-\frac{V_{ocn}-V_{mp}}{I_{mp}} \quad (9)$$

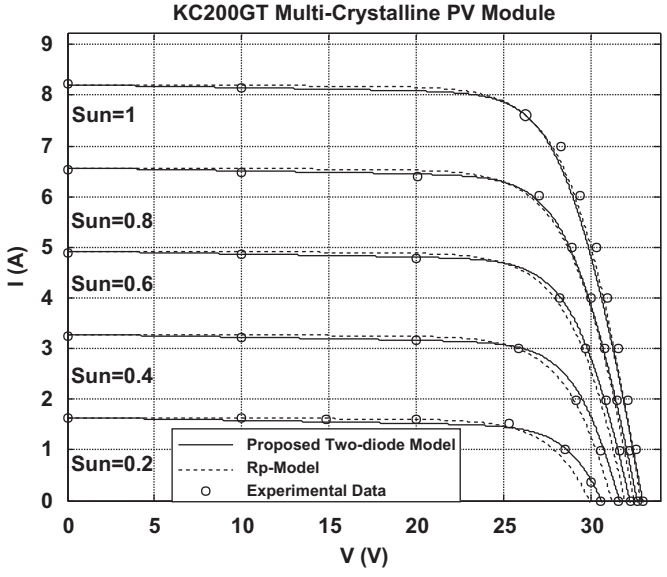

Fig. 7. I–V curves of R_p-model and proposed two-diode model of the KC200GT PV module for several irradiation levels at 25 °C.

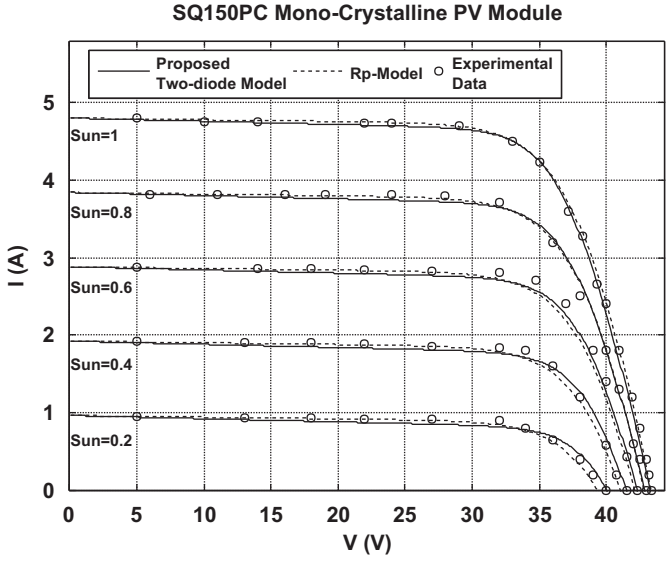

Fig. 8. I–V curves of R_p and proposed two-diode model of the SQ150-PC PV module for several irradiation levels at 25 °C.

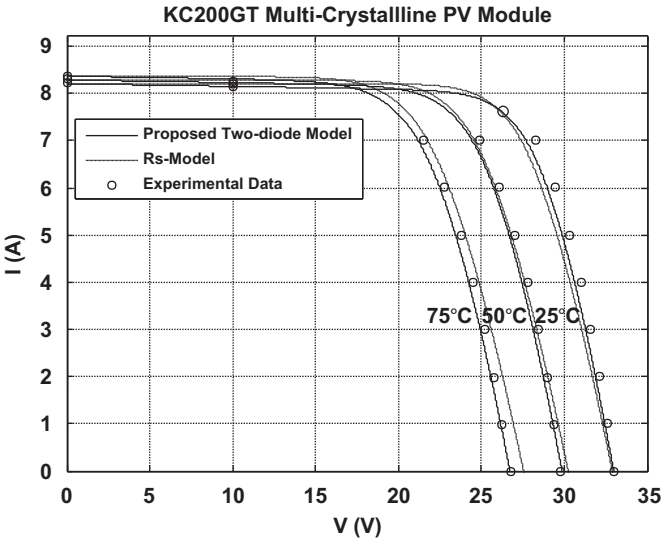

Fig. 9. The I–V curves of R_s and proposed two-diode model of the KC200GT PV module for several temperature levels at 1 KW/m^2.

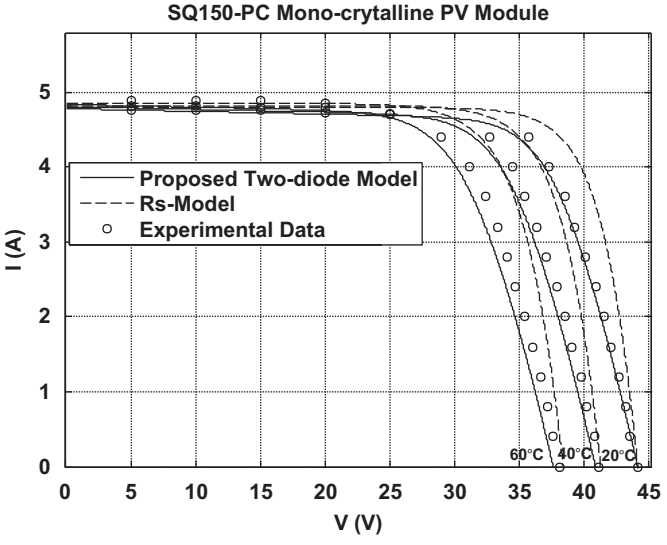

Fig. 10. I–V curves of R_s and proposed two-diode model of the SQ150-PC PV module for several temperature levels at 1 KW/m^2.

The initial value of R_p is the slope of the line segment between short-circuit and the maximum power points. For every iteration, the value of R_p is calculated simultaneously using Eq. (8). With the availability of all the six parameters, the output current of the cell can now be determined using the standard Newton–Raphson method. The flowchart that describes the P_{mp} matching algorithm is given in Fig. 6.

Using Eqs. (4) and (6), all the four parameters of this model can be readily computed, i.e. I_{PV}, I_o, R_p and R_s. From these, only R_p and R_s need to be determined by iteration. I_{PV} and I_o are obtained analytically. Variable p can be chosen to be any number value greater than 2.2.

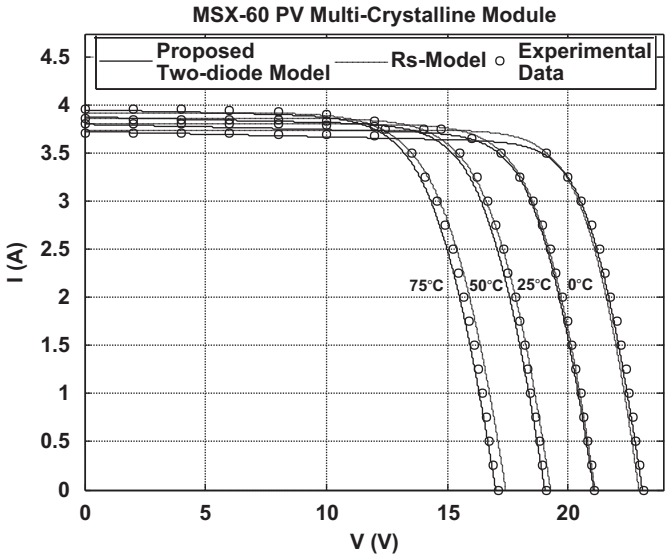

Fig. 11. The I–V curves of R_s and proposed two-diode model of the MSX-60 PV module for several temperature levels at 1 KW/m^2.

3. Results and discussion

3.1. Simulation and experimental results

The modeling methods described in this paper are validated by measured parameters of selected PV modules. The experimental (V, I) data are extracted from the manufacturer's datasheet and from [12] and [8]. Six different modules of different brands/models are utilized for verification; these include the multi- and mono-crystalline as well as thin-film types. The specifications of the modules are summarized in Table 1.

Table 2 shows the parameters used for the R_s-model. Four parameters are calculated namely, I_o, I_{PV}, ideality factor a and R_s. In the R_p-model shown in Table 3, the additional calculated parameter is the shunt resistance; R_p. Table 4 shows the parameters for the proposed two-diode model. Although the model has more variables, the actual number of parameters computed is four because $I_{o1}=I_{o1}=I_o$ while $a_1=1$ and p can be chosen arbitrarily, i.e. $p \geq 2.2$.

Figs. 7 and 8 show the I–V curves for KC200GT [31,32] and SQ150-PC [32,33], respectively, for different levels of irradiation (per unit Sun=1 equivalent to 1000 W/m^2). The calculated values from the proposed two-diode and R_p-models are evaluated against measured data from the manufacturer's datasheet. Comparison to the R_s-model is not included in the plot to avoid overcrowding of traces. However, the results for the R_s-model will be shown later in the performance analysis between the three models.

The proposed two-diode model and the R_p-model exhibit similar results at STC. This is to be expected because both models use the similar max power matching algorithm to evaluate the

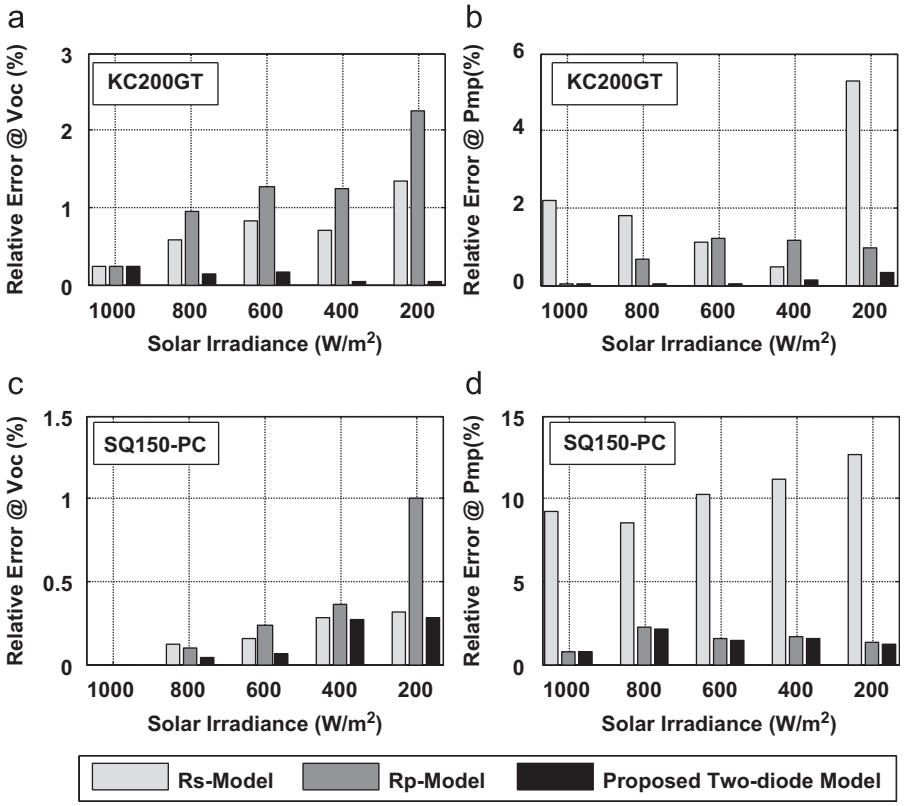

Fig. 12. Relative error for V_{oc} and P_{mp}, for R_s, R_p and the proposed two-diode model for (a,b) KC200GT and (c,d) SQ150-PC PV modules.

model parameters at STC. However, at low irradiance, more accurate results are obtained from the proposed model, especially in the vicinity of the open circuit voltage. At V_{oc}, the R_p-model shows departure from the experimental data, suggesting that R_p-model is inadequate when dealing with low irradiance level. It is envisaged that this will have significant implication during partial shading. Similar trend is observed for the SQ150-PC module.

The performance of the models when subjected to temperature variation is considered next. All measurements are conducted at STC irradiance of 1000 W/m^2. The proposed model is compared to the R_s-model to highlight the problems with the latter when subjected to temperature variations. The R_p-model is not shown for simplicity, but will be included later in the analysis that compares all the three models together.

For all the three modules tested (KC200GT, SQ150-PC, MSX-60 [33,34]), it can be seen that both the proposed and R_p-models have approximately equivalent performance at STC temperature (25 °C). However at higher temperature, results from the R_s-model

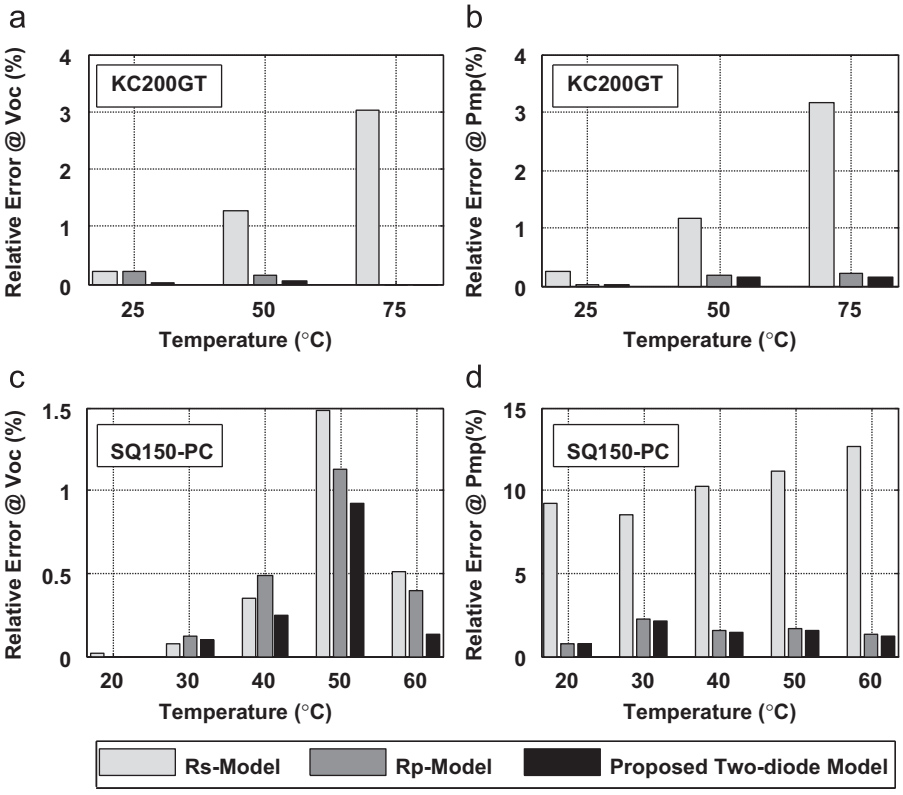

Fig. 13. Relative error for V_{oc} and P_{mp}, for R_s, R_p and the proposed two-diode model for (a,b) KC200GT and (c,d) SQ150-PC PV modules.

Table 5
Relative errors on the M_{pp} of R_s, R_p and proposed two-diode model at different temperature for S36 (multi-crystalline) module.

Temp (°C)	Measured data	R_s-model	R_p-model	Two-diode model	Error R_s (%)	Error R_p (%)	Error two-D (%)
50	P_{mp}=31.95	P_{mp}=35.02	P_{mp}=31.83	P_{mp}=31.90	9.608 at P_{mp}	0.219 at P_{mp}	0.156 at P_{mp}
	V_{mp}=14.60	V_{mp}=16.18	V_{mp}=14.90	V_{mp}=14.80	10.82 at V_{mp}	2.055 at V_{mp}	1.369 at V_{mp}
25	P_{mp}=36.00	P_{mp}=39.08	P_{mp}=36.10	P_{mp}=35.90	8.556 at P_{mp}	0.278 at P_{mp}	0.278 at P_{mp}
	V_{mp}=16.50	V_{mp}=18.05	V_{mp}=16.80	V_{mp}=16.70	9.393 at V_{mp}	1.818 at V_{mp}	1.212 at V_{mp}
0	P_{mp}=40.05	P_{mp}=43.08	P_{mp}=40.31	P_{mp}=40.09	7.565 at P_{mp}	0.649 at P_{mp}	0.099 at P_{mp}
	V_{mp}=18.40	V_{mp}=19.93	V_{mp}=18.80	V_{mp}=18.70	8.315 at V_{mp}	2.174 at V_{mp}	1.630 at V_{mp}
−25	P_{mp}=44.10	P_{mp}=47.01	P_{mp}=44.56	P_{mp}=44.17	6.559 at P_{mp}	1.043 at P_{mp}	0.158 at P_{mp}
	V_{mp}=20.30	V_{mp}=21.83	V_{mp}=20.60	V_{mp}=20.35	7.537 at V_{mp}	1.478 at V_{mp}	0.246 at V_{mp}

Table 6
Relative errors on the M_{pp} of R_s, R_p and proposed two-diode model at different temperature for SP-70 (mono-crystalline) module.

Temp (°C)	Measured Data	R_s-Model	R_p-Model	Two-Diode Model	Error R_s (%)	Error R_p (%)	Error Two-D (%)
50	P_{mp}=62.13	P_{MP}=63.81	P_{mp}=61.75	P_{mp}=61.89	1.690 at P_{mp}	0.612 at P_{mp}	0.386 at P_{mp}
	V_{mp}=14.60	V_{mp}=14.91	V_{mp}=14.60	V_{mp}=14.60	2.123 at V_{mp}	0.000 at V_{mp}	0.000 at V_{mp}
25	P_{mp}=70.00	P_{mp}=72.14	P_{mp}=69.99	P_{mp}=69.99	3.057 at P_{mp}	0.014 at P_{mp}	0.014 at P_{mp}
	V_{mp}=16.50	V_{mp}=16.72	V_{mp}=16.50	V_{mp}=16.50	1.333 at V_{mp}	0.000 at V_{mp}	0.000 at V_{mp}
0	P_{mp}=77.88	P_{mp}=80.46	P_{mp}=78.19	P_{mp}=77.91	3.313 at P_{mp}	0.393 at P_{mp}	0.038 at P_{mp}
	V_{mp}=18.40	V_{mp}=18.57	V_{mp}=18.50	V_{mp}=18.50	0.924 at V_{mp}	0.543 at V_{mp}	0.543 at V_{mp}
−25	P_{mp}=85.75	P_{mp}=88.72	P_{mp}=86.32	P_{mp}=85.70	3.464 at P_{mp}	0.665 at P_{mp}	0.058 at P_{mp}
	V_{mp}=20.30	V_{mp}=20.44	V_{mp}=20.50	V_{mp}=20.50	0.690 at V_{mp}	0.985 at V_{mp}	0.985 at V_{mp}

deviate from the measured values significantly, as shown in Figs. 9 and 10, respectively. However for MSX-60 module shown in Fig. 11, both the proposed and the R_s-model accurately fit the experimental data for all temperature conditions. The accuracy of the R_s-model in this particular case can be attributed to the fact that the R_s-model is originally developed and verified using the MSX-60 module [5].

Fig. 12(a), (b) and (c), (d) shows the analysis for relative error of V_{oc} and the P_{mp} for KC200GT and SQ150-PC modules at different irradiance levels. The temperature is set to STC. The relative error is defined as the difference between simulated and measured V_{oc} and P_{mp} values. The difference is then divided by the measured value. As can be seen at STC irradiance, there is a very small difference in the V_{oc} values among the three models. However as the irradiance is reduced, there is a significant deviation of V_{oc} calculated using the R_s and R_p-models. Similar results can be observed for the P_{mp}. On the other hand, the proposed two-diode model accurately calculates P_{mp} at all irradiance values.

Fig. 13(a), (b) and (c), (d) shows the performance of the three models when subjected to variation in module temperature. There is no significant difference between the R_p and the two-diode models. However the R_s-model exhibits poor performance for both V_{oc} and P_{mp} calculations.

To show the effectiveness of the models for different silicon technology, comparisons between S36 (mono-crystalline), SP-70 (multi-crystalline) and ST40 (thin-film) are carried out. Tables 5–7 show the relative errors for V_{mp} and P_{mp} for a wide variation of temperature ($-25\,^{\circ}C$ to $+50\,^{\circ}C$). The irradiance is maintained constant at STC. From the data it can be concluded, more accurate results are obtained from the two-diode model for the all three silicon technologies. Furthermore it can be noted that using the R_s-model, considerable errors occur for V_{mp} and P_{mp}. This is

Table 7
Relative errors on the M_{pp} of R_s, R_p and proposed two-diode model at different temperatures for ST40 (thin-film) module.

Temp (°C)	Measured data	R_s-model	R_p-model	2-diode model	Error R_s (%)	Error R_p (%)	Error two-D (%)
50	$P_{mp}=34.00$	$P_{mp}=43.77$	$P_{mp}=33.69$	$P_{mp}=33.71$	28.73 at P_{mp}	0.912 at P_{mp}	0.853 at P_{mp}
	$V_{mp}=14.10$	$V_{mp}=17.68$	$V_{mp}=14.30$	$V_{mp}=14.20$	25.39 at V_{mp}	1.418 at V_{mp}	0.709 at V_{mp}
25	$P_{mp}=40.00$	$P_{mp}=48.52$	$P_{mp}=40.00$	$P_{mp}=40.00$	21.30 at P_{mp}	0.000 at P_{mp}	0.000 at P_{mp}
	$V_{mp}=16.60$	$V_{mp}=19.41$	$V_{mp}=16.60$	$V_{mp}=16.60$	25.39 at V_{mp}	0.000 at V_{mp}	0.000 at V_{mp}
0	$P_{mp}=46.00$	$P_{mp}=53.30$	$P_{mp}=46.42$	$P_{mp}=46.33$	15.87 at P_{mp}	1.605 at P_{mp}	0.717 at P_{mp}
	$V_{mp}=19.10$	$V_{mp}=21.16$	$V_{mp}=19.10$	$V_{mp}=19.10$	10.78 at V_{mp}	0.000 at V_{mp}	0.000 at V_{mp}
−25	$P_{mp}=52.00$	$P_{mp}=58.10$	$P_{mp}=52.92$	$P_{mp}=52.69$	11.73 at P_{mp}	1.769 at P_{mp}	0.442 at P_{mp}
	$V_{mp}=21.60$	$V_{mp}=22.92$	$V_{mp}=21.60$	$V_{mp}=21.60$	6.111 at V_{mp}	0.000 at V_{mp}	0.000 at V_{mp}

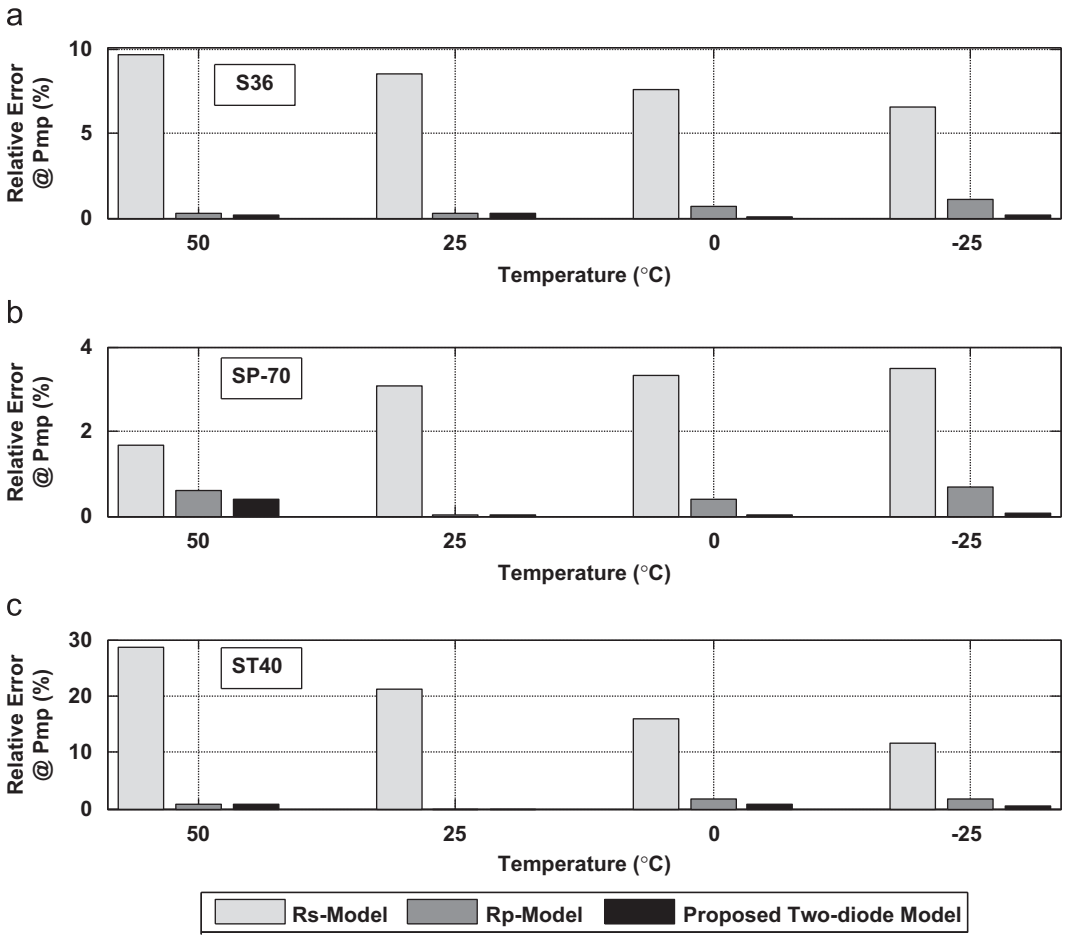

Fig. 14. Relative error for P_{mp} of R_s, R_p and the proposed two-diode model for temperature variation (a) S36 (multi-crystalline) (b) SP-70 (mono-crystalline) and (c) ST40 (thin-film).

particularly severe for the thin film technology. For clarity, the P_{mp} data in Tables 5–7 are plotted in Fig. 14(a)–(c), respectively.

4. Conclusion

In this paper, an improved two-diode modeling method for PV module is described. Unlike the previous similar models suggested by other researchers, the proposed work requires the computation of only four parameters. In addition, a simple and fast iterative approach is employed to compute the series and parallel resistances. The accuracy of the proposed model is evaluated using practical data from the manufacturers of six PV modules of different types. Its performances are compared to the popular single diode R_s and R_p-models. It was found that in all cases, the proposed model is superior when subjected to irradiance and temperature variations. In particular, it exhibits excellent accuracy at lower irradiance conditions. It is envisaged that the proposed model can be a valuable design tool for PV system designers.

Acknowledgment

The authors would like to thank Universiti Teknologi Malaysia for providing the facilities and research grant to conduct this research.

References

[1] S. Roundy, P.K. Wright, J.M. Rabaey, Energy Scavenging for Wireless Sensor Networks: With Special Focus On Vibrations, first ed., Kluwer Academic Publishers, Norwell, MA, 2004.
[2] Y.T. Tan, D.S. Kirschen, N. Jenkins, A model of PV generation suitable for stability analysis, IEEE Trans. Energy Convers. 19 (4) (2004) 748–755.
[3] A. Kajihara, A.T. Harakawa, Model of photovoltaic cell circuits under partial shading, in: Proceedings of the IEEE International Conference on Industrial Technology (ICIT), 2005, pp. 866–870.
[4] W. Xiao, W.G. Dunford, A. Capel, A novel modeling method for photovoltaic cells, in: Proceedings of the IEEE 35th Annual Power Electronics Specialists Conference (PESC), 2004, pp. 1950–1956.
[5] G. Walker, Evaluating MPPT converter topologies using a matlab PV model, J. Electr. Electron. Eng., Australia 21 (1) (2001) 45–55.
[6] K. Khouzam, L. Cuong, K.K. Chen, N.Y. Poo, Simulation and real time modeling of space photovoltaic systems, in: Proceedings of the IEEE First World Conference Photovoltaic Energy Conversion, Conference Record 24th IEEE Photovoltaic Specialists Conference, 1994, pp. 2038–2041.
[7] E. Matagne, R. Chenni, R. El Bachtiri, A photovoltaic cell model based on nominal data only, in: Proceedings of International Conference Power Engineering, Energy Electrical Drives, POWERENG, 2007, pp. 562–565.
[8] R. Chenni, M. Makhlouf, T. Kerbache, A. Bouzid, A detailed modeling method for photovoltaic cells, Energy 32 (2007) 1724–1730.
[9] S. Liu, R.A. Dougal, Dynamic multiphysics model for solar array, IEEE Trans. Energy Convers. 17 (2) (2002) 285–294.
[10] M. Chegaar, Z. Ouennoughi, A. Hoffmann, A new method for evaluating illuminated solar cell parameters, Solid State Electron. 45 (2001) 293–296.
[11] D. Sera, R. Teodorescu, P. Rodriguez, PV panel model based on datasheet values, in: Proceedings of the IEEE International Symposium on Industrial Electronics (ISIE), 2007, pp. 2392–2396.
[12] M.G. Villalva, J.R. Gazoli, E.R. Filho, Comprehensive approach to modeling and simulation of photovoltaic arrays, IEEE Trans. power electron. 24 (5) (2009) 1198–1208.
[13] C. Sah, R.N. Noyce, W. Shockley, Carrier generation and recombination in p–n junctions and p–n junction characteristics, in: Proceedings of IRE, 45 1957, pp. 1228–1243.
[14] T.F. Elshatter, M.E. Elhagree, Aboueldahab, A.A. Elkousry, Fuzzy modeling and simulation of photovoltaic system, in: Proceedings of the 14th European Photovoltaic Solar Energy Conference, 1997.
[15] M. Balzani, A. Reatti, Neural network based model of a PV array for the optimum performance of PV system, Res. Microelectron. Electron., IEEE 2 (2005) 123–126.
[16] A. Mellit, M. Benghanem, S.A. Kalogirou, Modeling and simulation of a stand-alone photovoltaic system using an adaptive artificial neural network, Renew. Energy 32 (2007) 285–313.
[17] E. Karatepe, M. Boztepe, M. Colak, Neural network based solar cell model, Energy Convers. Manage. 47 (2006) 1159–1178.
[18] E. Syafaruddin, Karatepe, T. Hiyama, Development of real-time simulator based on intelligent techniques for maximum power point controller of PV modules, The Int. J. Innovative Comput. Inf. Control (IJICIC) 6 (2010) pp. 1623–1642.
[19] F. Almonacid, C. Rus, L. Hontoria, M. Fuentes, G. Nofuentes, Characterization of Si-Crystalline PV module by artificial neural networks. A comparative study with other methods, Renew. Energy 35 (2010) 973–980.
[20] F. Almonacid, C. Rus, L. Hontoria, F.J. Munoz, Characterization of PV CIS module by artificial neural networks. A comparative study with other methods, Renew. Energy 35 (2010) 973–980.
[21] J.A. Gow, C.D. Manning, Development of a photovoltaic array model for use in power-electronics simulation studies, IEEE Proc. Electr. Power Appl. 146 (1999) 193–200.
[22] J.A. Gow, C.D. Manning, Development of a model for photovoltaic arrays suitable for use in simulation studies of solar energy conversion systems, in: Proceedings of the Sixth International Conference on Power Electronics Variable Speed Drives, 1996, pp. 69–74.
[23] S. Chowdhury, G.A. Taylor, S.P. Chowdhury, A.K. Saha, Y.H. Song, Modelling, simulation and performance analysis of a PV array in an embedded environment, in: Proceedings of the 42nd International Conference on Universities Power Engineering (UPEC), 2007, pp. 781–785.
[24] A. Hovinen, Fitting of the solar cell IV-curve to the two diode model, Physica Scr. 54 (1994) 175–176.
[25] J. Hyvarinen, J. Karila, New analysis method for crystalline silicon cells, in: Proceedings of the Third World Conference on Photovoltaic Energy Conversion, 2003, pp. 1521–1524.
[26] K. Kurobe, H. Matsunami, New two-diode model for detailed analysis of multicrystalline silicon solar cells, Jpn. J. Appl. Phys. 44 (2005) 8314–8321.
[27] K. Nishioka, N. Sakitani, K. Kurobe, Y. Yamamoto, Y. Ishikawa, Y. Uraoka, T. Fuyuki, Analysis of the temperature characteristics in polycrystalline Si solar cells using modified equivalent circuit model, Jpn. J. Appl. Phys. 42 (2003) 7175–7179.
[28] K. Nishioka, N. Sakitani, Y. Uraoka, T. Fuyuki, Analysis of multicrystalline silicon solar cells by modified 3-diode equivalent circuit model taking leakage current through periphery into consideration, Sol. Energy Mater. Sol. Cells 91 (2007) 1222–1227.
[29] K.R. McIntosh, P.P. Altermatt, G. Heiser, Depletion-region recombination in silicon solar cells: when does mDR=2?, in: Proceedings of the 16th European photovoltaic Solar Energy Conference 2000, pp. 251–254.
[30] N. Enebish, D. Agchbayar, S. Dorjkhand, D. Baatar, I. Ylemj, Numerical analysis of solar cell current–voltage characteristics, Sol. Energy Mater. Sol. Cells 29 (1993) 201–208.
[31] C. Sah, Fundamentals of solid-state electronics, World Scientific Publishing Co. Pvt. Ltd., Singapore, 1991.
[32] KC200 GT High Efficiency Multicrystal Photovoltaic Module Datasheet Kyocera. [Online]. Available: 〈http://www.kyocera.com.sg/products/solar/pdf/kc200gt.pdf〉.
[33] Shell Solar Product Information Sheet [Online]. Available: 〈http://www.solarcellsales.com/techinfo/technical_docs.cfm〉.
[34] Solarex MSX60 and MSX64 Solar Arrays Datasheet. (1997). [Online]. Available: 〈http://www.californiasolarcenter.org/newssh/pdfs/solarex-MSX64.pdf〉.